Arab Journal of Nuclear Science and Applications, 48(4), (76-87) 2015

Investigation of Induced Force Distribution Profiles in Coaxial Plasma Device

H.A. EL-Sayed, T.M. Allam and H.M. Soliman
Plasma Physics and Nuclear Fusion Dept., Nuclear Research Center, AEA, Cairo, Egypt

Received: 10/12/2014 **Accepted: 5/2/2015**

ABSTRACT

This paper presents the results of the experimental investigations of the axial distribution of magnetic and electric forces profiles. Moreover, is decreases the theoretical estimation of radial and axial plasma current sheath density along the inter electrode discharge region of a 1.5 KJ coaxial Nitrogen plasma discharge device with negative inner electrode polarity. All the data are taken at the average value of inner and outer electrodes radii and along the coaxial electrodes. Maxwell's equations are used in the present work.

This device is energized by a condenser bank of 30 μf capacity with charging voltage of 10 KV and the discharge is operated with Nitrogen gas of a pressure ranging from 1 to 2.2 Torr. This system delivers a peak discharge current of 56 KA with a periodic time of 32 μs. Dependence of Nitrogen gas pressures on the maximum value of different magnetic and electric forces which affect the Plasma Current Sheath (PCS) motion in different directions of (r, θ, z) and during the axial phase are discussed to get the optimum discharge conditions to operate the coaxial plasma device under consideration. Also the effect of N_2 gas pressure on the helical performance of PCS motion is studied at different axial distances along the coaxial electrodes.

Key words: Coaxial Discharge, Electric Force, Magnetic Force, Plasma Current Sheath.

INTRODUCTION

Coaxial plasma discharge devices are used to inject plasma at a high velocity into different types of magnetic confinement devices[1-4].Also, they are important to study the plasma dynamics [5-7]. Furthermore, they are used in plasma application fields such as a deposition process [8] and for relativistic electron beam interaction studies [9].

In general, the coaxial plasma discharge dynamics is accomplished by two main phases: (1) the formation of axis-symmetric current sheath at the insulator surface between coaxial electrodes breech, and the plasma current sheath, PCS lifts off the insulator surface by $(J \times B)_r$ force where, J and B are the PCS density and magnetic field induction, respectively, (2) the axial phase, where the current sheath with an axial symmetry is formed, which is then accelerated up by $(J \times B)_z$ force towards the opened end of coaxial electrodes muzzle [10].

In order to get a general view of plasma current sheath dynamics along the coaxial electrodes system of coaxial plasma discharge device, it is important to investigate the magnetic and electric fields which affecting the plasma current sheath motion during the axial phase.

Several studies were made in the past to detect the behavior of induced magnetic fields induction associated with plasma current sheath during the axial propagation. Some of them are presented here [11-13]. In a coaxial plasma focus device of 4.4 kJ, the experimental results of magnetic forces distribution profiles showed that they depend on the Helium gas pressure[11]. Previous experimental works on coaxial plasma gun (67 kJ – 20 kV), have shown that, a magnetic field which is trapped ahead of current sheath will reduce the high ejection rate of plasma. This reduction should

lead to more uniform plasma [12]. Experimental results of the azimuthal magnetic field induction behind the PCS along the coaxial electrodes system of 2.8 kJ coaxial plasma focus device, showed that the magnetic field is increased with the axial distance along the annular space between the coaxial electrodes [13].

The magnetic probe offers a simple and cost-effective diagnostic tool that is generally used to measure the arrival time of the current sheet, the magnitude of the azimuthal magnetic field and the axial magnetic field distribution profiles of the current sheet in the initial phase [14] as well as the axial acceleration phase [15 – 17].

Al-Hawat [18] used a magnetic probe in analyzing the current sheath in plasma focus device with energy of about 2.8 KJ. Two magnetic probes are used in these studies for 1 mbar filling of argon. The axial distribution of trajectory, average axial velocity, and magnetic field of the current sheath at a certain radial distance along the axis of the tube were obtained experimentally and compared with numerical analysis from the snow plow model for the axial phase. The arrival time of the current sheath at the end of the anode (16 cm) is similar for both of the magnetic probes and gives an average velocity of the current sheath equal to 1.52 cm/μs.

Gurey et al. [19] studied current sheath by magnetic probes on PF-400 and detected toroidal vortexes and repeated current sheaths, indicating a complicated picture of current flow in plasma focus discharge.

The polarity of the inner electrode, IE, has a significant effect on the focus action. With negative IE Decker [20] managed to get focus action giving a high neutron yield by shielding off the radial electric field.

The main purpose of the present paper is to study the maximum value of magnetic and electric forces affecting on plasma current sheath propagation at different directions of *(r, θ, z)* during the axial phase of coaxial plasma discharge device operated with Nitrogen gas.

The experimental results are taken from an average of 5 shots at least for every discharge condition under consideration.

EXPERIMENTAL SETUP

The coaxial plasma discharge device used in this work and details of the device have been reported elsewhere[21]. It consists of two coaxial stainless steel electrodes, an outer electrode OE and an inner electrode IE of 60 cm and 13 cm lengths and diameters of 8.9 cm and 5 cm, respectively. A Teflon insulator ring is placed between the IE and the OE at the coaxial electrodes breech. This device is powered by a capacitor bank of 30 μf, charged up to 14 kV. Then a high discharge current of 56 KA is delivered from the capacitor bank and passes through the two coaxial electrodes via a spark gap switch and 12 coaxial cables which causes a generation of plasma sheath at the coaxial electrodes breech.

The IE has a negative polarity until defocus condition is detected [22]. The discharge takes place in nitrogen gas with an operating pressure ranging from 1 to 2.2 Torr. The pertinent features of the coaxial plasma discharge device are shown schematically in figure 1. Also the electrical circuit of our device is presented in figure 2.

A resistive voltage divider consisting of ten pieces of 560 Ω and terminated by a 56 Ω (division ratio of 100) is connected across the anode and cathode. It records the HV transients at the breech end of the discharge coaxial device. A Rogowski coil of 150 turns and calibration factor of 68 KA/v is fixed around one of the coaxial cables to record the discharge current. It is connected to the scope via a passive integrator of time constant RC = 7×10^{-3} s. Typical oscilloscopic trace for the HV probe and Rogowski coil for p = 2.2 Torr are shown in figure 3.

A magnetic probe with 36 turns of enameled copper wire of 2.8 mm diameter, cross section area of 6.38×10^{-2} cm^2 and calibration factor of 0.35 KG/v is used to detect the plasma sheath behavior along the coaxial electrodes via measurements of azimuthal and axial components, B_θ and B_z of the magnetic field induction attached with PCS. The probe is inserted in the annular space between the two electrodes at radial distance equal the average radius of inner and outer electrodes, r = 0.035 m. Measurements are made as a function of the axial position as z varies from z = 2 cm to z = 11 cm (z = 0 at the breech and z =11 cm at the muzzle), and also as a function of pressure.

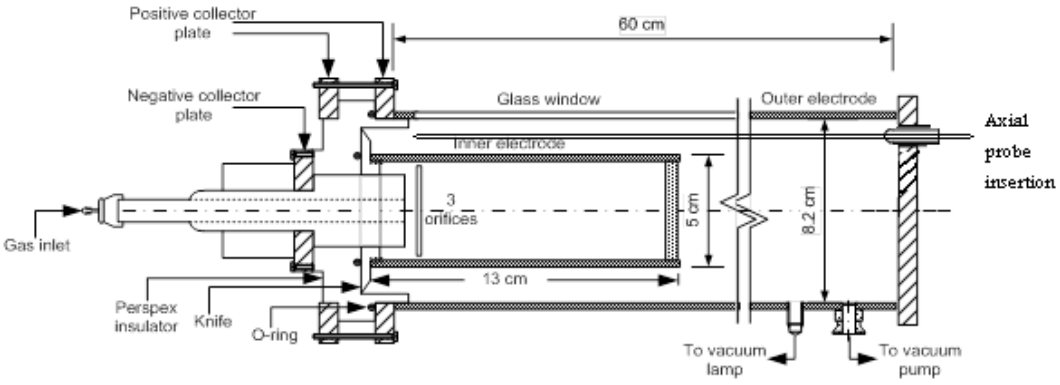

Fig. (1): Coaxial plasma discharge device.

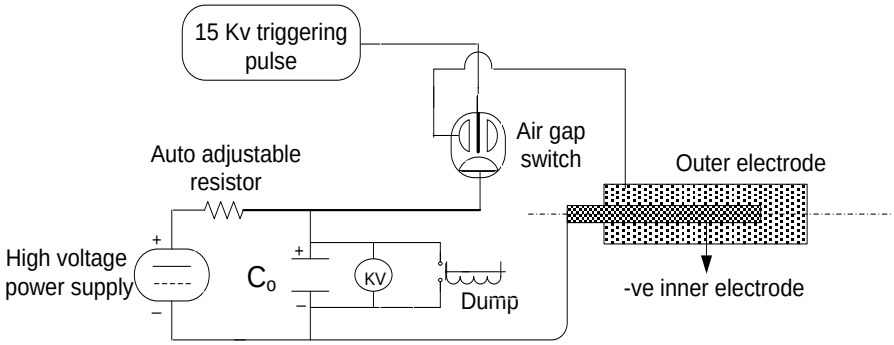

Fig. (2): Electrical circuit of the coaxial plasma discharge device.

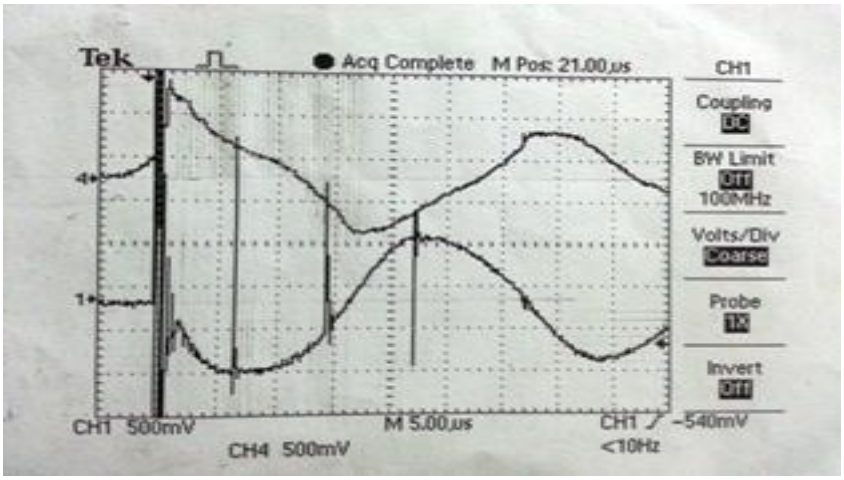

Fig. (3): Oscilloscopic signals of I_{dis} "Lower trace" and V_{dis} " Upper trace"At p = 2.2 Torr

RESULTS AND DISCUSSION

In this paper, the maximum value of the electric and magnetic forces affecting the PCS propagation during the axial phase is studied to investigate a general view of coaxial plasma discharge dynamics.

Results are divided into two sections: the first section deals with the axial distribution profiles of the radial and azimuthal electric forces / unit volume, $F_{r\ (elec.)}$ and $F_{\theta\ (elec.)}$ along the coaxial electrodes system and at radial distance, r = 3.475 cm. The second section is concerned with the axial, radial and azimuthal magnetic forces / unit volume $F_{z\ (mag.)}$, $F_{r\ (mag.)}$ and $F_{\theta(mag.)}$ along the coaxial electrodes and at the same radial distance mentioned above. Results of the two sections are obtained as a function of N_2 gas pressure within the range from 1 to 2.2 Torr.

Signals of magnetic probe in the axial and azimuthal directions with discharge current are shown in figure 4a and b. From the data obtained the space and time distribution of the magnetic field induction associated with the PCS in axial, B_z, azimuthal, B_θ, direction along the coaxial electrodes, (z -direction), the corresponding distribution of PCS density, J and the electric field, E can be calculated from the Maxwell's equations.

The experimental results are measured at different times ranging from 1.27 μs to 10.75 μs after the initial current discharge.

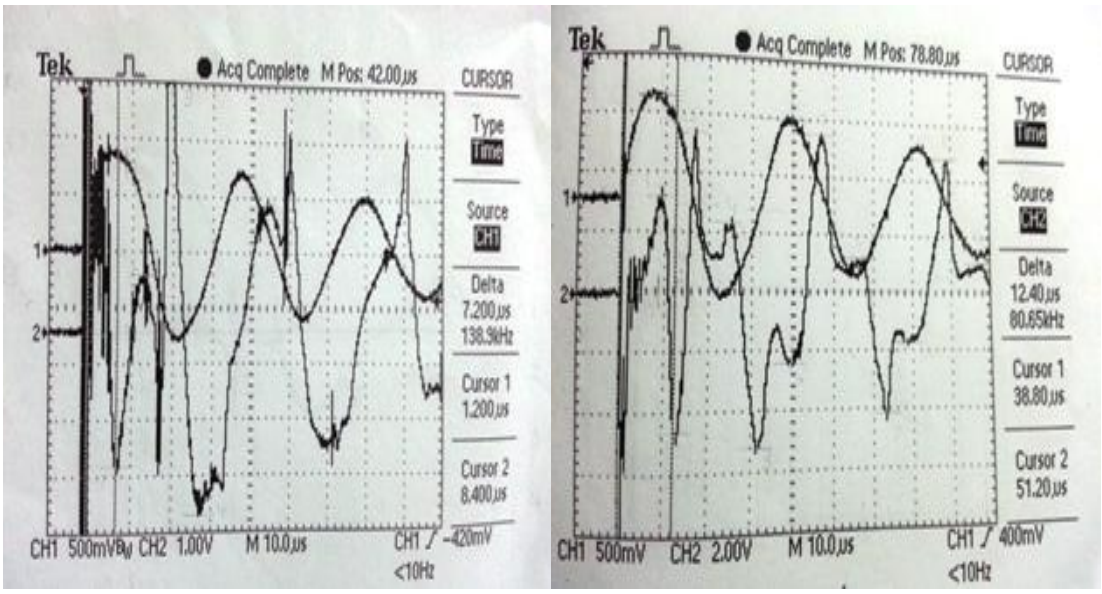

(a) **(b)**

(B_z)"Lower trace" and I_{dis} "Upper trace" At p = 1 Torr and z = 2 cm

(B_θ) "Lower trace" and I_{dis} "Upper trace" At p = 1.4 Torr and z = 8 cm

Fig. (4): Oscilloscopic signals of magnetic probe "Lower trace" and I_{dis} "Upper trace" for (a) axial direction and (b) azimuthal direction.

(A) Electric forces

Radial and azimuthal electric forces / unit volume, $F_{r\ (elec.)}$ and $F_{\theta\ (elec.)}$ are given by the following equations:

$$F_{r(elec)} = enE_r \quad (1)$$

and $$F_{\theta(elec)} = enE_\theta \quad (2)$$

where $n = \frac{\rho N_A}{A}$ is the number density for the gas,
N_A is the Avogadro's number
A is the atomic weight of the gas.
ρ is the gas density, in our work we take a single ionized case, where:
$n = n_e = n_i \; and \; \rho = \rho_e = \rho_i$

Radial[23] and azimuthal[24] electric fields, E_r and E_θ, are given, respectively, by:

$$E_r = {}^{V_{dis}}/_{rln(b/a)} \qquad (3)$$

where V_{dis} is the discharge voltage which measured by the high voltage probe.
a and b are the radius of inner and outer electrode respectively.

$$E_\theta = \frac{r}{c}\frac{\partial B_z}{\partial t} \qquad (4)$$

Figure 5 shows the variation of E_r with axial distance, z, at different N_2 gas pressures. This figure shows that E_r gradually decreases with the increase in z and its maximum value = 95.58 × 10^3 V/m is detected at p = 2.2 Torr and z = 0.02 m. Figure 6 shows the relation between E_θ and z for different gas pressures, this relation has approximately the same relation of E_r with z. $E_\theta(max)$ =9.06 × 10^2 V/m at z = 0.02 m and p = 2.2 Torr.

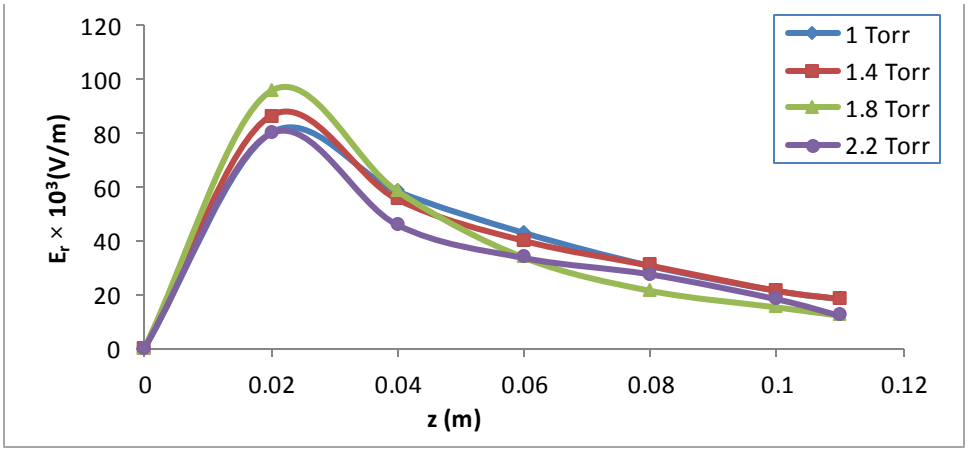

Fig. (5): Variation of E_r with z at different N_2 gas pressures.

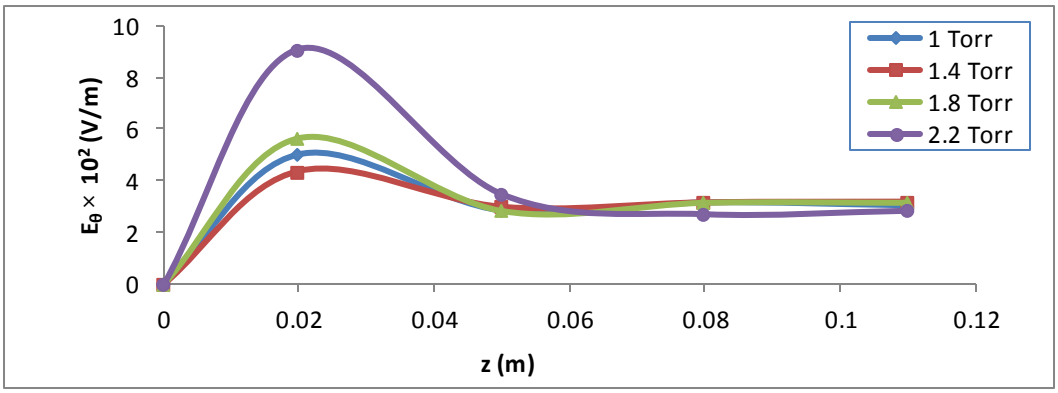

Fig. (6): Variation of E_θ with z at different N_2 gas pressures.

Dependence of $F_{r\ (elec.)}$ and $F_{\theta\ (elec.)}$ on axial distance z and at different gas pressures are illustrated in figures 7 and 8 respectively. An interesting result has been found that the $F_r \rangle\rangle F_\theta$ along the coaxial electrodes, i.e., the effect of $F_{\theta\ (elec.)}$ on PCS motion is approximately neglected with respect to the effect of $F_{r\ (elec.)}$.

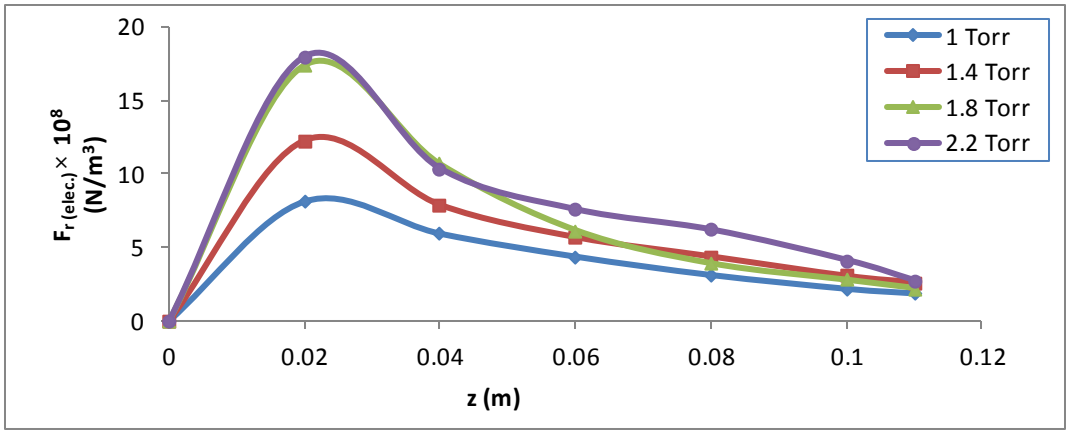

Fig. (7): Radial electric force / unit volume versus axial distance, z at different gas pressures.

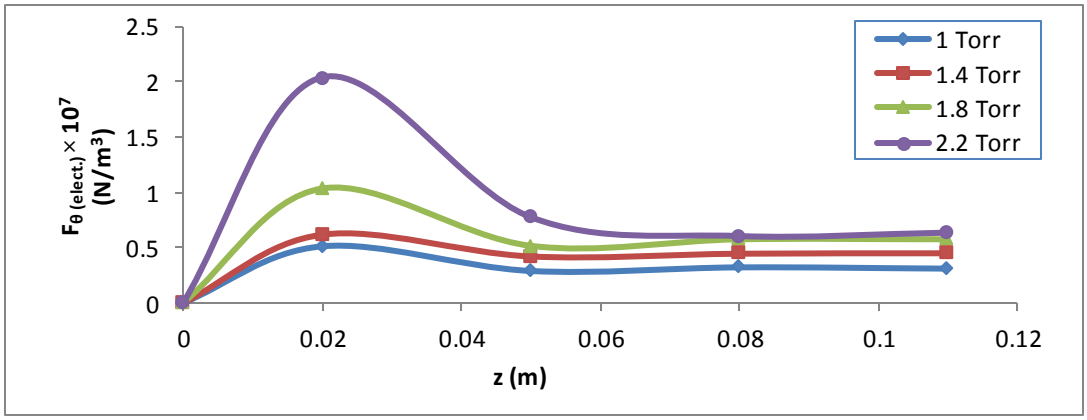

Fig. (8): Azimuthal electric force/unit volume versus axial distance, z at different gas pressures.

Figure 9 shows the variation of $F_{r\ (elec.)}$ with N_2 gas pressure at different axial distances, z. As it is evident from this figure, the effect of N_2 gas pressure on $F_{r\ (elec.)}$ is observed clearly at distance closes to coaxial electrodes breech, however it decreases with increasing of axial distance ,i.e., at the coaxial electrodes muzzle (end of coaxial electrodes) $F_{r\ (elec.)}$ is approximately has a constant value for all gas pressures under consideration.

(B) Magnetic Forces

The axial, radial and azimuthal magnetic force / unit volume along the coaxial electrodes and at fixed r = 0.035 m are given, respectively, by:

$$\left.\begin{aligned} F_{z(mag)} &= (J \times B)_z = J_r B_\theta - J_\theta B_r \\ F_{r(mag)} &= (J \times B)_r = J_\theta B_z - J_z B_\theta \\ F_{\theta(mag)} &= (J \times B)_\theta = J_z B_r - J_r B_z \end{aligned}\right\} \qquad (5)$$

Neglecting magnetic field induction in radial direction, B_r and the PCS density in azimuthal direction, J_θ for simplicity, then

$$F_{z(mag)} = J_r B_\theta \ , \ F_{r(mag)} = J_z B_\theta \ \ and \ \ F_{\theta(mag)} = J_r B_z$$

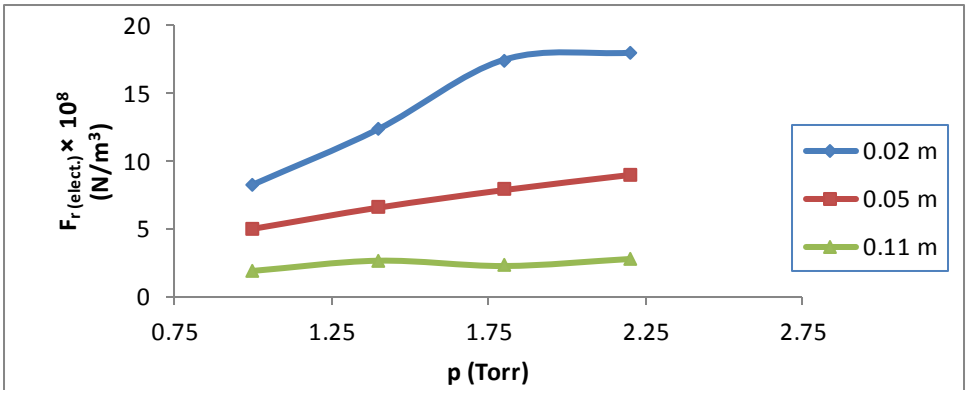

Fig. (9): Radial electric force / unit volume versus N_2 gas pressures at different axial distances.

Where J_r and J_z are the radial and axial PCS density, B_θ and B_z are the azimuthal and axial magnetic fields induction associated with PCS.

J_r and J_z are evaluated by the following Maxwell's equations and our assumption mentioned above are applied, then:

$$J_r = -\frac{c}{4\pi}\left(\frac{\partial E_r}{c\partial t} + \frac{\partial B_\theta}{\partial z}\right) \quad \text{, and} \tag{6}$$

$$J_z \cong \frac{c}{4\pi r} B_\theta \tag{7}$$

Figures (10 and 11) illustrate the variation of J_r and J_z with axial distance, z for different N_2 gas pressures respectively. These figures demonstrate that at pressure of 1 and 1.4 Torr J_r is increased gradually with increasing axial distance along the coaxial electrodes. At gas pressure of 2.2 Torr J_r is decreased slightly with z. Also J_z is approximately decreased from a distance nearly to breech until the muzzle for p = 1 and 1.4 Torr, while at p = 2.2 Torr it increased from breech to 0.08 m afterwards it decreased with axial distance. In general these results cleared that, at p = 2.2 Torr a decrease of PCS density at axial distance near the coaxial electrodes muzzle may be due to current shedding effect or particles collisions process of high plasma density.

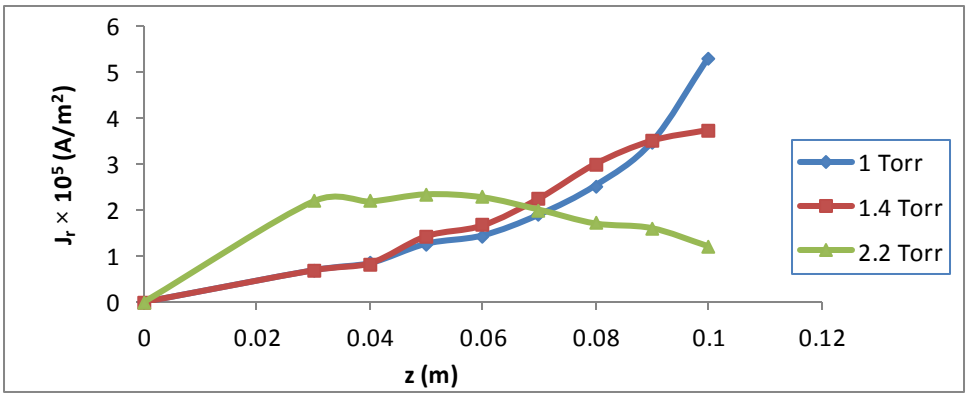

Fig. (10): Radial plasma current sheath density versus axial distance at different N_2 gas pressures.

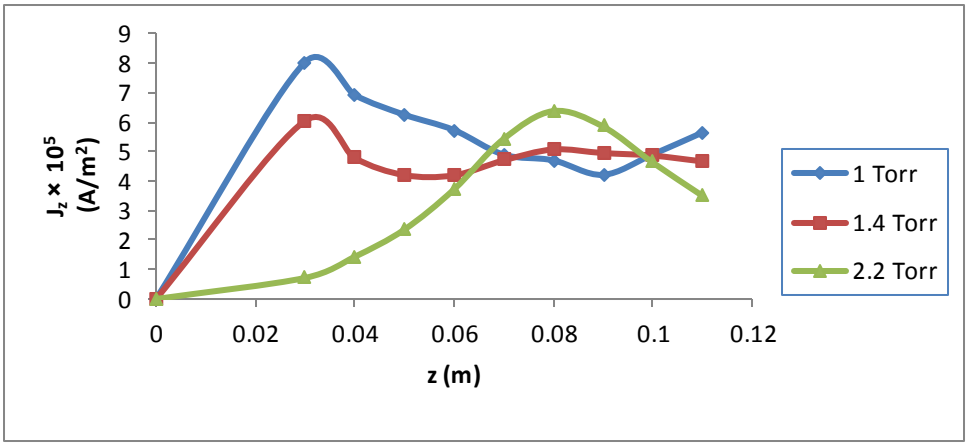

Fig. (11): Axial plasma current sheath density versus axial distance at different N_2 gas pressures.

Variation of axial magnetic force / unit volume, F_z as a function of axial distance z at different N_2 gas pressures is shown in figure 12. It can be seen from the figure that, at p = 1 and 1.4 Torr, F_z has the same behavior and it increased with z, while at p = 2.2 Torr F_z is increased until z = 0.07 m, then it decreased with z like that observed with J_r and J_z data. The maximum value of F_z at coaxial electrodes muzzle = 1.134×10^4 N/m^3 is obtained at p = 1 Torr.

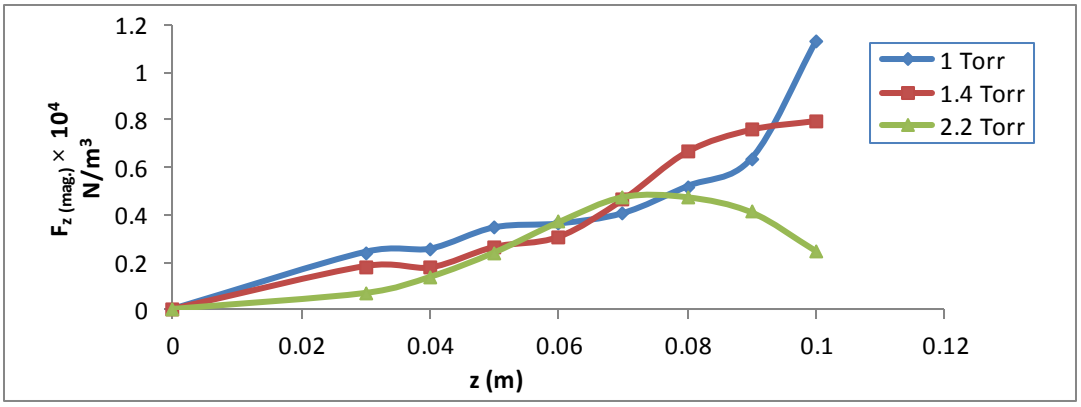

Fig. (12): Variation of axial magnetic force / unit volume with axial distance at different N_2 gas pressures

Figure 13 represents the relation between $F_{r\,(mag.)}$ versus axial distance and at different N_2 gas pressures. As it is evident from this figure, the axial distribution of $F_{r\,(mag.)}$ has the same distribution profiles for p = 1 and 1.4 Torr

(F_r is approximately decreased with axial distance, z from z = 0.03 m to coaxial electrodes muzzle) while at p = 2.2 Torr it has a vise verse behavior for most axial distances (from z = 0.03 m to 0.08 m) afterwards it decreased until z = 0.11 m, like the same results of $F_{z\,(mag.)}$. The maximum value of $F_{r\,(mag.)}$ at coaxial electrodes muzzle = 1.39×10^4 N/m^3 for p = 1 Torr.

Variation of $F_{\theta\,(mag.)}$ with axial distance and at different N_2gas pressures is shown in figure 14. This figure verifies that $F_{\theta\,(mag.)}$ versus z at p = 1 and 1.4 Torr has the same behavior and it increased gradually with axial distance but at p = 2.2 Torr, the above relation has a vise versa behavior, from z = 0.03 m to 0.10 m. The maximum value of $F_{\theta\,(mag.)}$ at the muzzle = 2.27×10^4 N/m^3 for p = 1 Torr.

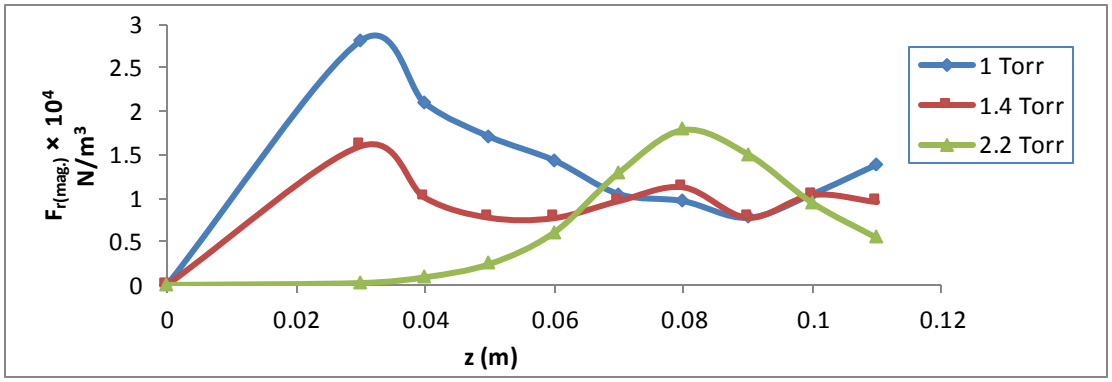

Fig. (13): Variation of radial magnetic force / unit volume with axial distance at different N_2 gas Pressures

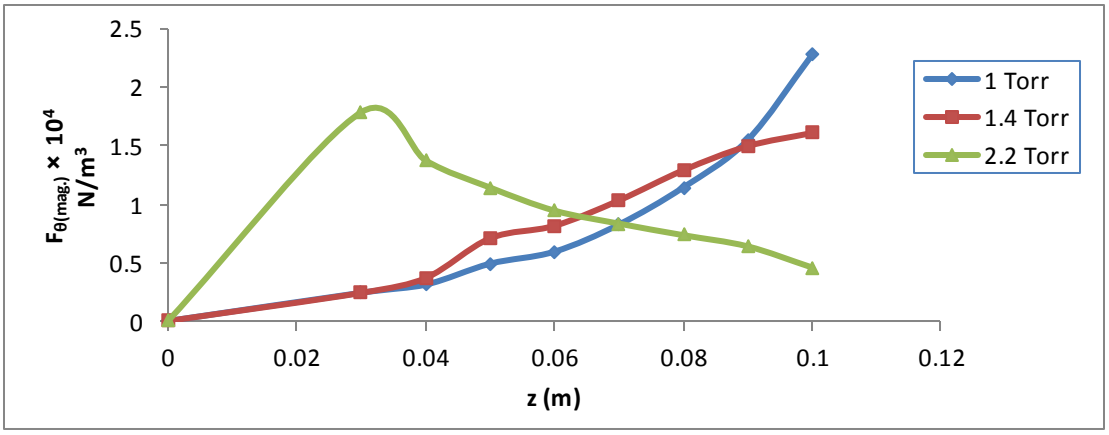

Fig. (14): Azimuthal magnetic force / unit volume versus axial distance at different N_2 gas pressures.

Figure 15 a, b, c shows the dependence of axial, radial and azimuthal magnetic forces / unit volume on N_2 gas pressures and at coaxial muzzle z = 0.10 m, mid distance between breech and muzzle, z = 0.05 m and at distance closes to breech, z = 0.03 m. The rate of change of $F_{z\,(mag.)}$, $F_{r\,(mag.)}$ and $F_{\theta\,(mag.)}$ data with N_2 gas pressure are listed in Table1. These data illustrate that the effect of changing N_2 gas pressures on $F_{z\,(mag.)}$ and $F_{\theta\,(mag.)}$ values is clear at the coaxial electrodes muzzle, and on $F_{r\,(mag.)}$ at the distance closes to coaxial electrodes breech. Also from the axial distribution of $F_{\theta\,(mag.)}$ and $F_{z\,(mag.)}$ as a function of N_2 gas pressures, it is observed that, the magnetic helicity which is detected from $\left(F_{\theta(mag)}/F_{z(mag)}\right)$ plays a role in the axial PCS dynamics along coaxial electrodes. The helicity motion is detected clearly at axial a distance close to coaxial electrodes breech, z = 0.03 m, t = 4.33 μs and p = 2.2 Torr and then it decreases with decreasing of gas pressure until p = 1 Torr, z = 0.03 m and t = 4.38 μs. the same behavior is repeated for z = 0.05 m, the helicity motion is clear at t = 6.67 μs and p = 2.2 Torr and it decreases with decreasing pressure until p = 1 Torr

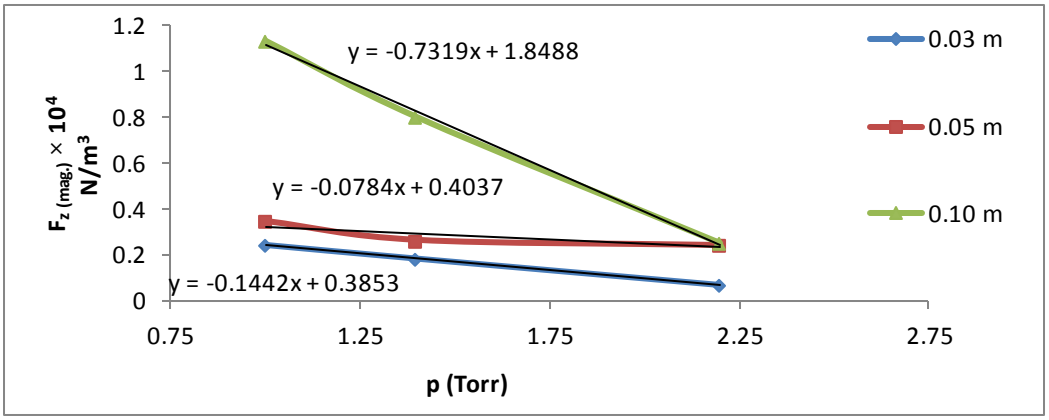

(a)

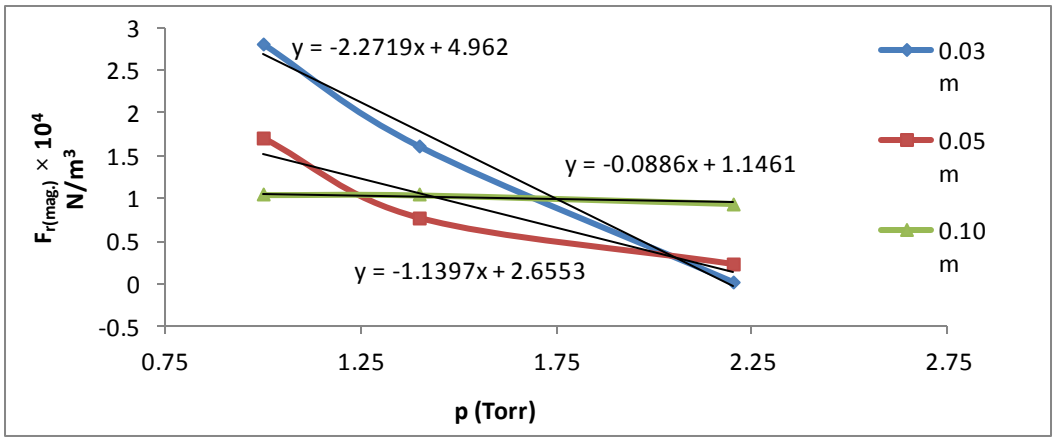

(b)

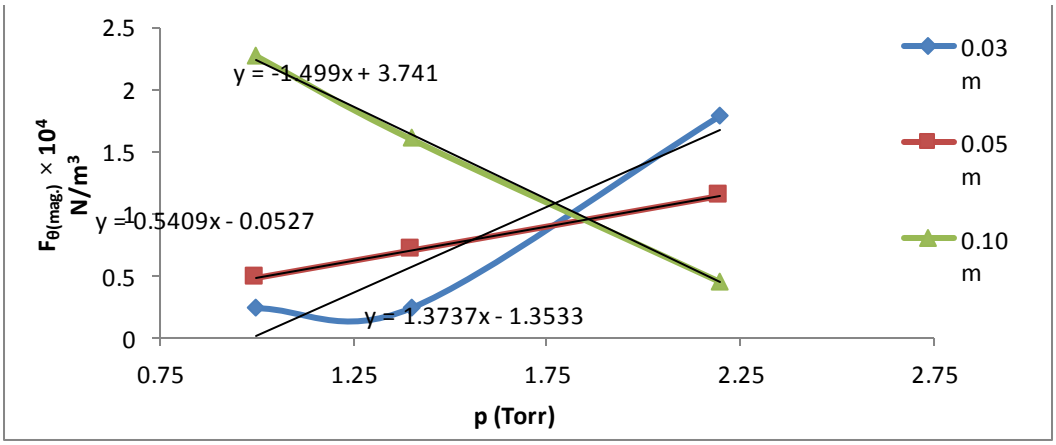

(c)

Fig. (15): a, b, c : Axial, radial and azimuthal magnetic force / unit volume versus N_2 gas pressure at different axial distances and t = 6.2 μs. At approximately the coaxial electrodes muzzle, at z = 0.10 m, the results show that, the changing of the N_2 gas pressures approximately doesn't affect the helicity motion of PCS.

Table (1): rate of change of magnetic forces data with N_2 gas pressures, (dF/dp) at different axial distances, z.

dF/dp	0.03 m	0.05 m	0.10 m
dF_z/dp	-0.144	-0.078	-0.731
dF_r/dp	-2.271	-1.139	-0.088
dF_θ/dp	1.373	0.54	-1.499

CONCLUSION

The results of radial and azimuthal electric fields indicate that they decrease slowly with the increase of axial distance along the coaxial electrodes and at different Nitrogen gas pressures.

It has been found that the radial electric force/unit volume is much greater than the azimuthal electric force/unit volume which in turn is nearly neglected. The effect of N_2 gas pressure on $F_{r\ (elec.)}$ is clear at a distance close to the coaxial electrodes breech and it is nearly constant at the electrodes muzzle, for all values of N_2 gas pressures.

The experimental results of radial and axial plasma current sheath density during the axial phase have been shown to depend on N_2 gas pressures. At high N_2 pressure of 2.2 Torr, a current shedding effect or particles collisions process may presented at z approaches to muzzle. The azimuthal and axial magnetic forces/ unit volume distribution profiles along the coaxial electrodes system have approximately the same behavior at N_2 gas pressures of 1 and 1.4 Torr, while the radial magnetic force/unit volume distribution along the coaxial electrodes (from z = 0.03 m to coaxial electrodes muzzle) has approximately a vise versa behavior at the same values of N_2 gas pressures. The maximum value of $F_{z\ (mag.)}$ and $F_{\theta\ (mag.)}$ is detected at p = 1 Torr and at coaxial electrodes muzzle. At p = 2.2 Torr, $F_{z\ (mag.)}$, $F_{r\ (mag.)}$ and $F_{\theta\ (mag.)}$ have approximately the same behavior along the coaxial electrodes, and their maximum values are located at z = 0.07 m, 0.08 m and 0.03 m, respectively. Results of $F_{z\ (mag.)}$ and $F_{\theta(mag.)}$ as a function of gas pressures show a reduction in helical motion of PCS along the coaxial electrodes which is detected at p = 1 Torr.

Finally, the optimum condition to operate our coaxial plasma device is found to be with N_2 gas pressure of 1 Torr.

REFERENCES

(1) D.G. Swanson, R.W. Clark, P. Korn, S. Rabertson, and C.B. Wharton, Phys. Rev. Lett. 28, 1015 (1972).

(2) A.W. Leonard, R.N. Dexter, J.C. Sportt, Phys. Fluids 30, 2877,(1987).

(3) D. J. Hoffman, J. N. Talmadge, and J. L. Sholat, Nucl. Fusion 21, 1130, (1981).

(4) S. F. Schaer, Acta Phys. Pol. A88 Supplement, S.77 (1995).

(5) Mei-Yu Wang, C.K. Choi, and F. B. Meadjr. AIP Conf. Proc. 246, 30, (1992).

(6) T. Ikehata, K. Qohashi, et al., Nucl. Instrum. Methods Phys. Kes. B 70, 26 (1992).

(7) T. M. Allam, H. A. El-Sayed, and H. M. Soliman "Plasma Current Sheath Motion in Coaxial Plasma Discharge" Journal of EPE vol. 3 no. 4 (2011).

(8) C. Kim, and D. F. Ogletree, Appl. Surf. Sci. 59, 261 (1992).

(9) S. K. Iyyengar, V. K. Rohatgi, Int. Conf. on Plasma Physics, vol. 3, p. 1165, (1989).

(10) Imshennik, N. Filippov and T. Filippova, Nuclear Fusion vol. 30 p. 929, (1973).

(11) G.M. El-Kashef and H. M.Soliman, "Magnetic Forces Distribution in a 4.4 KJ Plasma Focus Device" 1st Cairo Conference on Plasma Physics and Applications, vol. 34, (2003).

(12) J.W. Mather, P. J. Bottoms, J. P. Carpenter, A. H. Williams, and K. D. Ware, the Phys. Of Fluids, vol. 12, no. 11, 2343 (1969).

(13) Sharif Al-Hawat, IEEE transactions on Plasma Science, vol. 32, no. 2 (2004).

(14) H. Bruzzone and D. Grondona "Magnetic probe measurements of the initial phase in a plasma focus device" Plasma Phys. Control Fusion 39 1315-26 (1997).

(15) T.Y. Tou "Multislit streak camera investigation of plasma focus in the steady-state rundown phase" IEEE Trans. Plasma Sci. 23 870-3 (1995).

(16) S. P. Chow, S. Lee and B.C. Tan "Current sheath studies in a coaxial plasma focus gun" J. Plasma Phys. 8 21-33 (1972).

(17) M. Mathuthu, T.G. Zengeni and A.V. Gholap Phys. Plasmas 3, 4572-6 (1996).

(18) S. Al-Hawat, IEEE Trans. Plasma Sci. 32 2 (2004).

(19) A. Gurey, V. Nikulin, S. Polukhin, I. Volobuev, "Problems of atomic science and technology" Series Plasma Phys. 15 98-100, (2009).

(20) G. Decker, W. Kies and G. Pross, "Experimental solving the polarity riddle of the plasma focus" Phys. Lett., vol. 89A, no. 8, pp. 393-396, (1982).

(21) H.M. Hussien, T. M. Allam, H. A. El-Sayed, and H. M. Soliman" Characterization of 1.5 KJ Coaxial Plasma Discharge" Journal of Eng. And Applied Sci. Vol. 56, no. 4 PP. 315 – 329 (2009).

(22) H.M. Soliman and M. M. Masoud, 17th International Symposium on Rarefied gas dynamics, A, Vol.2, P. 479, (1991).

(23) Gang Shen – Zhi, J. Phip. D. Appl. Phys., 28, 314, (1994).

(24) S. Glaston and R. H. Lovberg, "Controlled Thermonuclear Reactions", Princton, Van Nostrand Co., Inc., (1960).